Available online at www.sciencedirect.com
ScienceDirect
Phytochemistry 69 (2008) 1573–1585
PHYTOCHEMISTRY
www.elsevier.com/locate/phytochem

Rhamnoarabinosyl and rhamnoarabinoarabinosyl side chains as structural features of coffee arabinogalactans

Fernando M. Nunes [a,*], Ana Reis [b], Artur M.S. Silva [b], M. Rosário M. Domingues [b], Manuel A. Coimbra [b]

[a] *Departamento de Química, Universidade de Trás-os-Montes e Alto Douro, P-5000-911 Vila Real, Portugal*
[b] *Departamento de Química, Universidade de Aveiro, P-3810-193 Aveiro, Portugal*

Received 6 November 2007; received in revised form 28 January 2008
Available online 17 March 2008

Abstract

The hot water soluble green coffee arabinogalactans, representing nearly 7% of total coffee bean arabinogalactans, were characterized by ^{1}H and ^{13}C NMR and, after partial acid hydrolysis, by ESI-MS/MS. Data obtained showed that these are highly branched type II arabinogalactans covalently linked to proteins (AGP), with a protein moiety containing 10% of 4-hydroxyproline residues. They possess a β-(1 → 3)-Gal*p*/β-(1 → 3,6)-Gal*p* ratio of 0.80, with a sugars composition of Rha:Ara:Gal of 0.25:1.0:1.5, and containing 2 mol% of glucuronic acid residues. Beyond the occurrence of single α-L-Ara*f* residues and [α-L-Ara*f*-(1 → 5)-α-L-Ara*f*-(1→] disaccharide residues as side chains, these AGPs contain unusual side chains at *O*-3 position of the β-(1 → 6)-linked galactopyranosyl residues composed by [α-L-Rha*p*-(1 → 5)-α-L-Ara*f*-(1→] and [α-L-Rha*p*-(1 → 5)-α-L-Ara*f*-(1 → 5)-α-L-Ara*f*-(1→] oligosaccharides. Rhamnoarabinosyl and rhamnoarabinoarabinosyl side chains are reported for the first time as structural features of plant arabinogalactan-proteins.

Keywords: Coffee; Polysaccharides; Oligosaccharides; AGP; NMR; Mass spectrometry

1. Introduction

Arabinogalactan-proteins (AGPs) are proteoglycans widely distributed throughout the plant kingdom (Sommer-Knudsen et al., 1998). They are present in the plasma membrane, within cell walls, and in the extracellular matrix (Ding and Zhu, 1997; Gao et al., 1999). The role of AGPs remains unclear, but they have been implicated in many processes of plant growth, development, or adaptation, such as cell proliferation (Serpe and Nothnagel, 1994; Thompson and Knox, 1998), cell expansion (Willats and Knox, 1996; Ding and Zhu, 1997), cell differentiation (Pennell and Roberts, 1990; Knox et al., 1991), and somatic embryogenesis (Thompson and Knox, 1998; Kreuger and van Holst, 1993; Chapman et al., 2000). AGPs are complex macromolecules due to their large, heterogeneous, and highly branched chains (Clarke et al., 1979).

Coffee beans are composed, approximately, by 15% of AGPs (Bradbury, 2001; Redgwell et al., 2002). The protein content of coffee AGPs has been reported to be 0.4–1.9% (Redgwell et al., 2002). Studies of the cell walls of green coffee bean endosperm using the AGP-specific β-glucosyl Yariv reagent and monoclonal antibodies have been shown that the AGPs have an widespread distribution across the cell walls as well as they present different structural forms in their arabinans in the region adjacent to the cell walls lumen (Sutherland et al., 2004).

Structural studies on coffee type II arabinogalactans, the carbohydrate moiety of AGPs, have shown that they are composed by a backbone of β-(1 → 3)-linked galactosyl residues, substituted at intervals in the *O*-6 position with various combinations of arabinosyl and galactosyl residues (Bradbury, 2001). Up to 10% of glucuronosyl residues occurred as non-reducing terminal units on (1 → 6)-linked

* Corresponding author. Tel.: +351 259 350273; fax: +351 259 350480.
E-mail address: fnunes@utad.pt (F.M. Nunes).

0031-9422/$ - see front matter © 2008 Elsevier Ltd. All rights reserved.
doi:10.1016/j.phytochem.2008.01.021

galactosyl side chains (Redgwell et al., 2002). The heterogeneity of the degree of branching and monosaccharide composition of the side chains turns green coffee AGPs an heterogeneous mixture.

Green coffee water soluble arabinogalactans have been extracted from ground coffee with hot water followed by dialysis purification. This procedure allowed to extract 1.1% of arabinogalactans in relation to the dry and defatted green coffee weight (Nunes and Coimbra, 2001). According to the literature values (Fischer et al., 2001), this amount of water soluble arabinogalactans can be estimated to be approximately 7% of the amount of green coffee bean arabinogalactans. Using graded ethanol precipitation, it was possible to obtain arabinogalactan fractions where the degree of branching and the amount of rhamnosyl residues increased with the increase of the concentration in ethanol. The major fraction (45%) of the water soluble arabinogalactans was recovered in the precipitate of a 75% ethanol solution (Nunes and Coimbra, 2001).

In order to highlight the structural features of coffee arabinogalactans, especially those loosely bound to cell walls, this work describes the purification and structural characterisation of the arabinogalactans present in the 75% ethanol insoluble fraction.

2. Results and discussion

2.1. Purification and general characterisation of coffee arabinogalactans

The sugars composition of the polysaccharides recovered in the 75% ethanol fraction (Et75) is shown in Table 1. Beyond the occurrence of Gal and Ara, Et75 also contains Man, Rha, and a minor amount of Glc. The presence of Man, as well as the detection, by methylation analysis (Table 2), of (1 → 4)-Man*p*, as well as (1 → 4,6)-, and terminally linked Man*p*, allows to infer the occurrence of a small amount of mannans (Nunes et al., 2005). The passage of the material by the anion-exchange on Q-Sepharose FF chromatographic media allowed to recover a not retained fraction (QSA) richer in sugars (Table 1) and presenting a glycosidic-linkage composition similar to the one of fraction Et75 (Table 2). As a consequence, the majority of the Et75 arabinogalactans (98%) were recovered in QSA fraction. Because the arabinogalactans from green coffee have higher molecular weight than galactomannans (Redgwell et al., 2002), the arabinogalactans were further fractionated by size exclusion chromatography on Sephacryl S-300 HR (Fig. 1), allowing to recover 37% of the applied material in fraction F1, near the column void volume (V_0), and 31% in a disperse lower molecular weight fraction (F2). From Fig. 1 it is possible to notice that a large amount of UV absorbing material was removed, although a small amount was still observed in F1. Sugars (Table 1) and methylation analysis (Table 2) of F1 and F2 fractions allowed to observe that the mannans were excluded from fraction F1, being the arabinogalactans the only polysaccharides present. Nevertheless, 80% of the rhamnosyl residues were recovered in F1 (Table 1) and by methylation analysis it was observed that they were exclusively terminally linked (Table 2). Although the results from uronic acid colorimetric analysis indicated a low amount of these residues and no (1 → 4)-Rha*p* residues were detected by methylation analysis, in order to exclude the hypothesis that these

Table 1
Yield and sugars composition[a] (g/100 g material) of the coffee arabinogalactan-rich fractions

	Yield (%)	Rha	Ara	Man	Gal	Glc	Total sugars
Et75	18[b]	1.49[d]	8.87	1.98	18.14	0.33	30.81
QSA	61[c]	3.18	16.46	3.11	24.13	0.51	47.39
F1	37[d]	6.64	25.18	0.31	44.50	–	76.63
F2	31[d]	1.98	26.21	8.99	24.19	1.05	62.42

[a] g Anhydrosugars/100 g material.
[b] g/100 g of the high molecular weight material.
[c] g/100 g of the Et75 fraction.
[d] g/100 g of the QSA fraction.

Table 2
Methylation analysis of coffee arabinogalactan-rich fractions

Linkage	Et75	QSA	F1	F2	Cell wall AGP[a]
T-Rha*p*	4.1	8.4	9.4	5.2	0–1.3
Total	4.1[b] (5)[c]	8.4 (7)	9.4 (9)	5.2 (3)	0.4–1.9
T-Ara*f*	18.1	19.8	16.6	30.4	17.7–23.0
T-Ara*p*	–	1.0	1.1	0.7	–
5-Ara*f*	14.3	14.3	20.1	13.3	3.1–9.9
3,5-Ara*f*	–	0.2	2.3		*t*–0.4
2,5-Ara*f*	–	2.0	–		0.8
Total	32.4 (33)	37.6 (39)	40.1 (37)	44.5 (47)	21.0–30.5
T-Man*p*	0.3	0.2	–	–	–
4-Man*p*	8.1	4.7	0.3	10.2	–
4,6-Man*p*	0.1	0.2	–	–	–
Total	8.5 (6)	5.1 (6)	0.3 (0.4)	10.2 (13)	–
T-Gal*p*	6.9	3.3	3.7	3.4	3.5–4.1
6-Gal*p*	2.6	2.2	2.4	1.9	1.6–2.5
3-Gal*p*	20.5	17.8	19.7	14.6	32.9–44.8
3,6-Gal*p*	24.6	21.9	24.5	18.5	24.1–25.1
Total	54.6 (55)	45.2 (47)	50.3 (54)	38.4 (35)	58.1–69.4
4-Glc*p*	0.7	1.3	–	1.7	–
Total	0.7 (1)	1.3 (1)	–	1.7 (2)	0.3–0.4
T-Glc*p*A	n.a.	1.2	n.a.	n.a.	
4-Glc*p*A	n.a.	1.1	n.a.	n.a	
Total	–	2.3	–	–	7.8–10.6

n.a.: not analysed.
[a] Glycosidic-linkage composition of green coffee arabinogalactans reported by Redgwell et al. (2002).
[b] Total molar percentage obtained by methylation analysis.
[c] Values in parenthesis are the molar percentage obtained by sugar analysis.

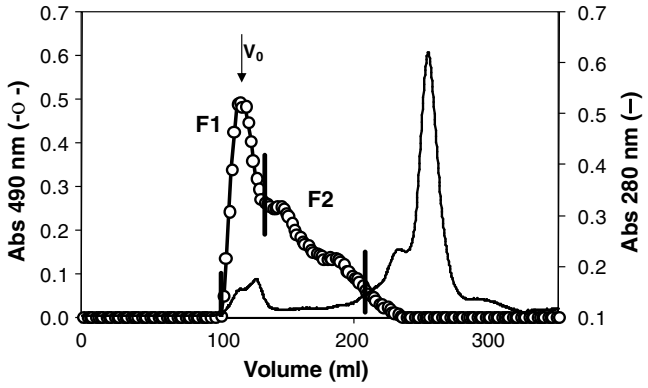

Fig. 1. Size exclusion chromatography of fraction Et75 of green coffee on Sephacryl-S 300 HR. Abs 490 nm from phenol to sulfuric acid carbohydrate analysis.

residues could belong to pectic polysaccharides (Redgwell et al., 2002), methanolysis of F1 fraction was performed. In the chromatograms shown in Fig. 2 for the direct methanolysis of fraction F1 (Fig. 2a), it is possible to observe the presence of glucuronic acid residues in an amount of nearly 2%. No galacturonic acid residues were detected. The absence of galacturonic acid residues confirms the absence of pectic polysaccharides in F1 fraction. Glucuronic acid residues are known to be a component of coffee arabinogalactans (Redgwell et al., 2002) as well as arabinogalactans from other origins (Clarke et al., 1979). However, the values found for this polysaccharide were very low when compared to the 7–10% that has been reported for coffee arabinogalactans (Redgwell et al., 2002). Although sugars like rhamnose, fucose, xylose, and mannose have always been detected in arabinogalactan-rich fractions, only in few cases these residues have been proved to be components of the arabinogalactans (Clarke et al., 1979).

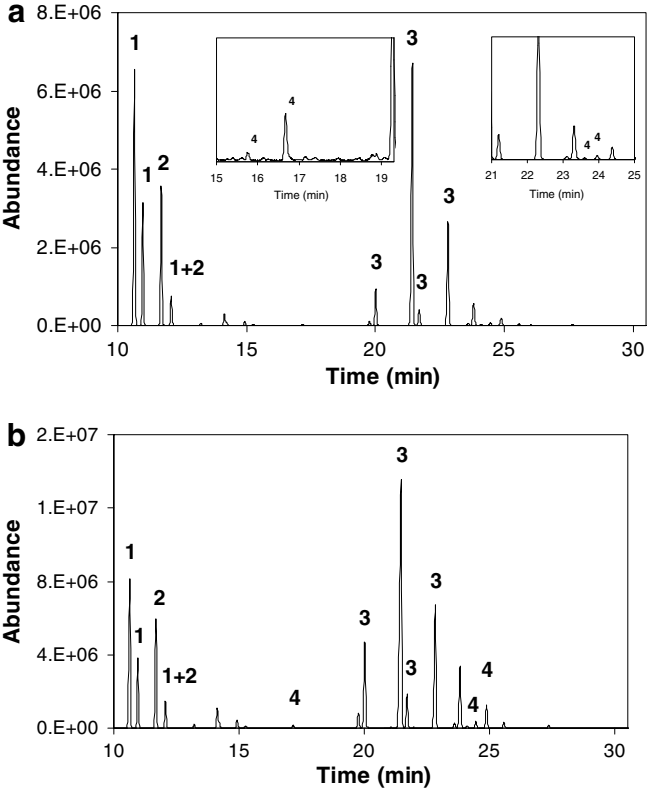

Fig. 2. Chromatographic profile of methanolysis products obtained from (a) fraction F1 and (b) fraction F1 after 50 mM partial acid hydrolysis. (1) arabinose (elution order α-*f* + β-*p*; α-*p* and β-*f*); (2) rhamnose (elution order α-*p* and β-*p*); (3) galactose (elution order α-*f*, α-*p*, β-*f*; and β-*p*); and (4) glucuronic acid (elution order α-*f* lactone, β-*f* lactone; β-*p* and α-*p*).

The arabinogalactans from coffee cell walls have been shown to be arabinogalactan-proteins (Redgwell et al., 2002). As during the purification the arabinogalactans presented absorption at 280 nm, it was performed an amino acid analysis of fraction F1 (Table 3). The amount of protein, estimated by the sum of all amino acid residues determined, was 4%, which, although in accordance with the amount of protein of other arabinogalactans (Sommer-Knudsen et al., 1998), was higher than that found for green coffee cell wall arabinogalactans (Redgwell et al., 2002). The amino acid composition of F1 was similar to that found for cell wall arabinogalactans from coffee (Table 3), with an higher abundance of Hyp residues, characteristic of arabinogalactans (Sommer-Knudsen et al., 1998; Josè-Estanyol and Puigdomènech, 2000). As the arabinogalactan-proteins are known to specifically bind the β-glycosyl-Yariv reagent, the material in F1 fraction was subjected to the single radial gel-diffusion method (van Holst and Clarke, 1985). The strong positive reaction given by the Yariv reagent, the co-purification of the protein with the carbohydrates, and its characteristic amino acid composition, allowed to conclude that the hot water soluble arabinogalactans are proteoglycans as those found for cell

Table 3
Amino acid composition (mol%) of F1 fraction from green coffee

	F1	Cell wall AGP[a]
Ala	12	11.6–17.9
Gly	10	8.3–11.4
Val	6	6.2–8.3
Thr	8	1.0–3.0
Ser	8	11.7–14.9
Leu	7	5.0–5.8
Ile	3	2.3–2.6
Pro	9	4.4–5.8
Hyp	10	7.0–12.6
Met	0	0.0–1.4
Asp	7	7.2–8.7
Phe	2	1.1–2.4
Glu	10	10.1–11.2
Lys	4	2.6–3.2
Tyr	1	1.6–5.9
Arg	2	0.7–2.4
His	–	0.3–0.8
Total[b]	4.22	0.4–1.9

[a] Amino acid composition of green coffee arabinogalactans reported by Redgwell et al. (2002).
[b] g Protein/100 g material.

wall arabinogalactan-proteins. In order to characterize in a more detail their carbohydrate structure, the polysaccharide moiety was further analysed by ESI-MS, ESI-MS/MS, and NMR.

2.2. ESI-MS and ESI-MS/MS analysis of coffee arabinogalactans

The polysaccharides of fraction F1 were submitted to a partial acid hydrolysis with 50 mM TFA. The material that eluted in the void volume (fraction A) on size exclusion chromatography on Biogel P-30 (Fig. 3a) was submitted to a stronger partial acid hydrolysis with 250 mM TFA (Fig. 3b). The low molecular weight products, fraction B from 50 mM TFA, and fraction A2 from 250 mM, were recovered and analysed by ESI-MS. Table 4 summarises the ions detected in the mass spectra of each fraction. For the 50 mM TFA partial hydrolysate, the ions observed at *m/z* 173, 305, 187, 319, and 451 can be attributed to the sodium adducts of pentose (Pent) and deoxyhexose (dHex) monomers, dimers, and trimers, namely $[Pent+Na]^+$, $[Pent_2+Na]^+$, $[dHex+Na]^+$, $[dHexPent+Na]^+$, and $[dHexPent_2+Na]^+$, respectively. Taking into account the sugars analysis of fraction F1, these results allow to conclude that the 50 mM partial hydrolysis released only arabinose and rhamnose monomers, Rha.Ara disaccharides, and

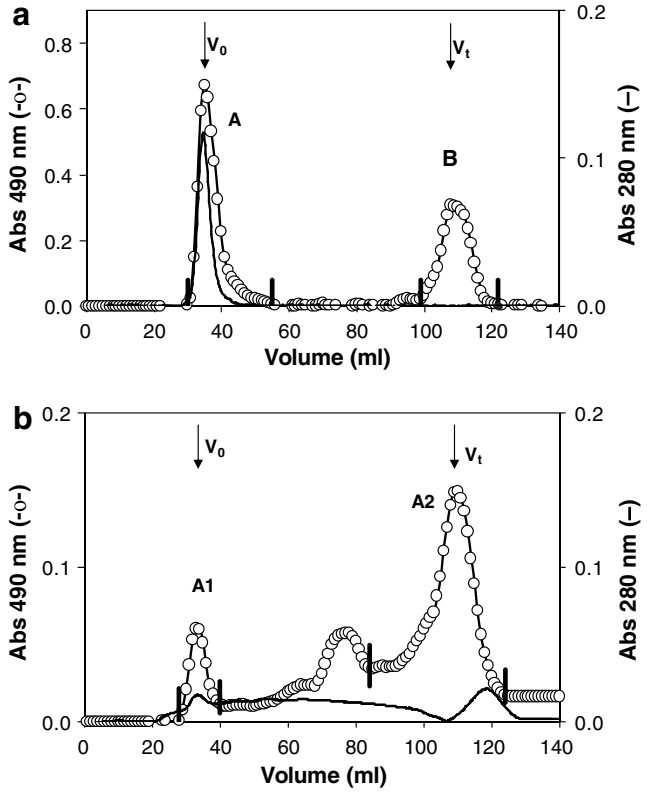

Fig. 3. Size exclusion chromatography on Biogel P-30 of the products obtained by partial hydrolysis of: (a) fraction F1 with 50 mM TFA and (b) peak A with 250 mM TFA. Abs 490 nm from phenol–sulfuric acid carbohydrate analysis.

Table 4
Summary of the oligosaccharide ions observed in the ESI-MS spectra of the low molecular weight partial hydrolysis products obtained from fraction F1

	Fraction B (TFA 50 mM)		Fraction A2 (TFA 250 mM)			
	$n=1$	$n=2$	$n=1$	$n=2$	$n=3$	$n=4$
Pentose containing oligosaccharides						
$[Pent_n+Na]^+$	173	305	173	–	–	–
$[Pent_2Hex+Na]^+$	–	–	467	–	–	–
$[PentHex_n+Na]^+$	–	–	–	497	659	821
Deoxyhexose containing oligosaccharides						
$[dHex_n+Na]^+$	187	–	187	–	–	–
$[dHexPent_n+Na]^+$	319	451	–	–	–	–
Uronic acid containing oligosaccharides						
$[HexAHex_n+Na]^+$	–	–	–	541	703	865
Hexose oligosaccharides						
$[Hex_n+Na]^+$	203	–	203	365	527	689

Rha.Ara_2 trisaccharides. This observation is in accordance with the results obtained for the methanolysis of the polymeric products resultant from the 50 mM partial hydrolysates (fraction A in Fig. 3a), where it is observed a decrease in the relative amount of arabinose and rhamnose residues (Fig. 2b). For the 250 mM TFA partial hydrolysate, the ions detected in the mass spectrum (Table 4) were attributed to the sodium adducts of Pent, dHex, and hexose (Hex) monomers, dimers, trimers, and tetramers of Hex_{2-4}, trimers, tetramers, and pentamers of $PentHex_{2-4}$, a trimer of $Pent_2Hex$, and trimers, tetramers, and pentamers containing uronic acid (HexA), $HexAHex_{2-4}$. The range of products formed in these two sequential partial hydrolysis is in accordance with the known relative acid stabilities (Selvendran and Ryden, 1990) of the glycosidic-linkages known to occur in type II arabinogalactans, as furanosyl linkages are more acid labile than pyranosyl linkages, and α-linkages are more acid labile than β-linkages. In order to confirm the proposed structures and obtain more structural information about their composition, the $[M+Na]^+$ ions were induced to fragment by collision with a gas (MS/MS).

Oligosaccharide fragment ions under ESI-MS/MS are the result of glycosidic cleavages between two sugar residues and of cross-ring cleavages (cleavage of two bonds within the sugar ring). The resulting fragments are usually named according to the nomenclature proposed by Domon and Costello (1988). Briefly, fragment ions that retain the charge at the non-reducing end are designated A when originated by cross-ring cleavages, or B and C when originated by glycosidic cleavage. The fragment ions that retain the charge at the reducing end are designated X when originated by cross-ring cleavages, or Y and Z when originated by glycosidic cleavage. Following the letter that defines the fragment type, there is a subscript that identifies the number of sugar residues in a linear oligosaccharide.

Structural information on the arabinosyl side chains was obtained by analysis of the ESI-MS/MS spectra of

$[Pent_2+Na]^+$ (*m/z* 305), $[Pent_2Hex+Na]^+$ (*m/z* 467), and $[PentHex_2+Na]^+$ (*m/z* 497) ions. For $[Pent_2+Na]^+$ (Fig. 4a), the predominant ions observed at *m/z* 173 and 155, attributed to the ions $[Pent+Na]^+$ and $[Pent_{res}+Na]^+$ formed by a C/Y-type and B/Z-type glycosidic bond cleavage, by the loss of a pentose residue and a pentose, respectively. Ions at *m/z* 245 and *m/z* 215 were attributed to $^{0,2}A_2$ and $^{0,3}A_2$ cross-ring fragments. A $^{2,4}X_1$ cross-ring cleavage could also explain the ion at *m/z* 215. However, the low energy collision induced dissociation (CID) product ion spectra show predominantly reducing end fragmentation (Zaia, 2004) allowing the attribution of this fragmentation to A cross-ring fragments. The loss of 60 and 90 Da from the precursor ion shows the occurrence of a terminally linked pentose residue at the *O*-5 position of the reducing end pentose, which is in accordance with the results of methylation analysis.

The MS/MS spectrum of ion *m/z* 467, attributed to $[Pent_2Hex+Na]^+$, is shown in Fig. 4b. The major fragment ion at *m/z* 335, attributed to $[PentHex+Na]^+$, was resultant from the loss of a pentose residue ($Pent_{res}$) from the precursor ion. Also observed with a high intensity was the ion at *m/z* 305, attributed to $[Pent_2+Na]^+$, resultant from a loss of 162 Da, that can be attributed to the loss of an hexose residue (Hex_{res}). The loss of 60, 90, and 120 Da from $[Pent_2Hex+Na]^+$, resulting in ions at *m/z* 407, 377, and 347, and from $[PentHex+Na]^+$, resulting in ions at *m/z* 275, 245, and 215, suggests that the reducing end hexose residue is substituted at the *O*-6 position. According to the sugars composition of fraction F1 it can be concluded

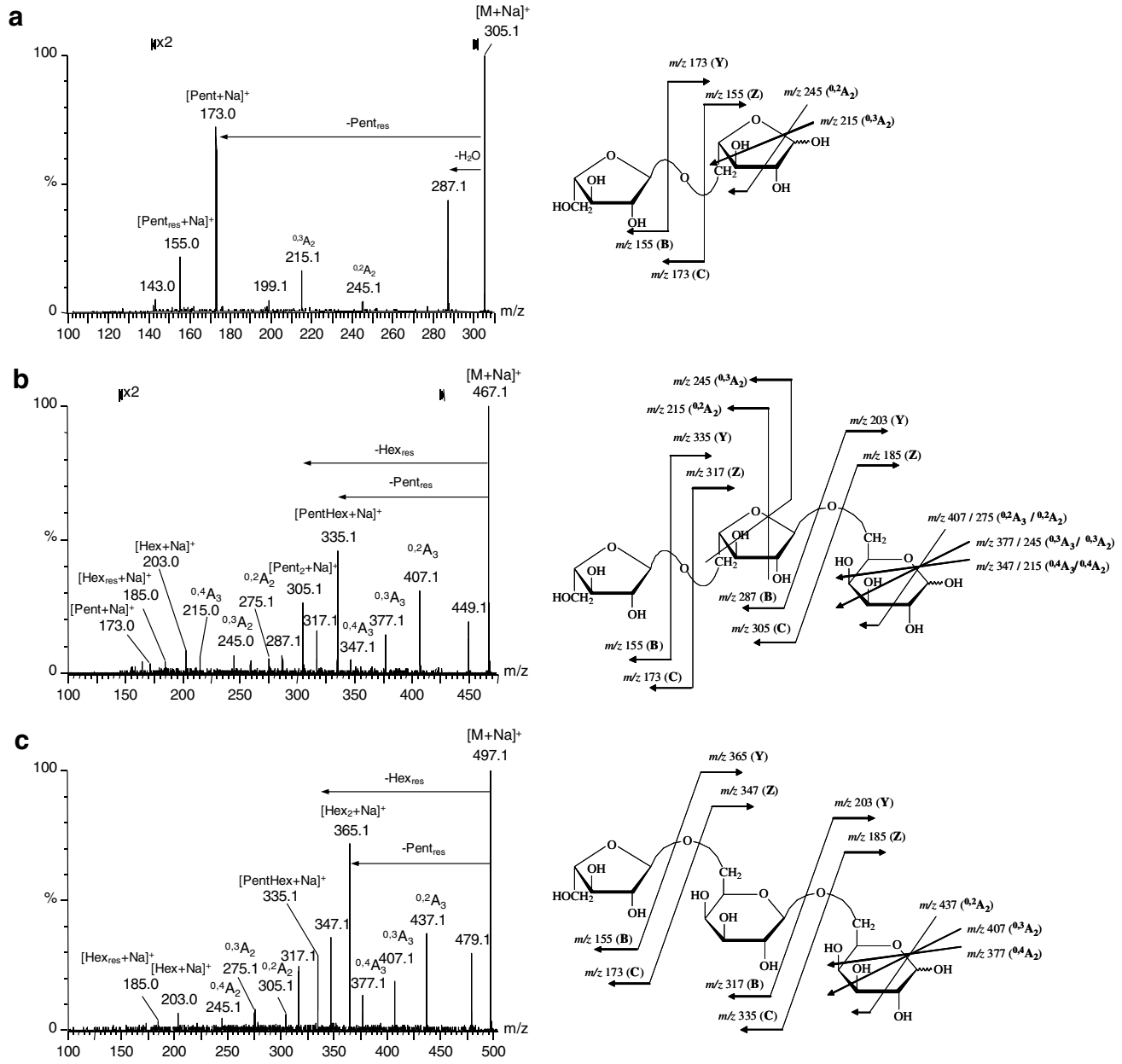

Fig. 4. ESI-MS/MS spectra of $[M+Na]^+$ adducts of (a) $Pent_2$, (b) $Pent_2Hex$ and (c) $PentHex_2$.

that these are arabinosyl disaccharides linked to the *O*-6 position of the galactosyl residues. Nevertheless, this result does not exclude the possible occurrence of arabinosyl disaccharides linked to the *O*-3 position of the reducing hexose residue. This is another possibility of linkage of the arabinose to the galactose residues, as their presence would result in a fragmentation pattern with a cross-ring cleavage with the loss of only 90 Da that would overlap with the fragmentation pattern observed.

The MS/MS spectrum of ion at *m/z* 497, attributed to $[PentHex_2+Na]^+$, is shown in Fig. 4c. The major fragment ion at *m/z* 365, attributed to $[Hex_2+Na]^+$, was resultant from the loss of the pentose residue, indicating that the two hexoses were linked to each other. Also observed with a high intensity was the ion at *m/z* 335, attributed to $[PentHex+Na]^+$, resultant from a loss of 162 Da that can be attributed to the loss of an hexose residue (Hex_{res}). The loss of 60, 90, and 120 Da from $[PentHex_2+Na]^+$, resulting in ions at *m/z* 437, 407, and 377, indicates that the reducing end hexose residue is substituted at the *O*-6 position (Simões et al., 2007).

The MS/MS spectrum of ion at *m/z* 541, attributed to $[HexAHex_2+Na]^+$, is shown in Fig. 5. The major fragment ion at *m/z* 365, attributed to $[Hex_2+Na]^+$, was resultant from the loss of an uronic acid residue ($HexA_{res}$). Also observed was the ion at *m/z* 379, attributed to $[HexAHex+Na]^+$, resultant from a loss of 162 Da, that can be attributed to the loss of an hexose residue (Hex_{res}). The ions at *m/z* 305, 275, and 245 were attributed to $^{0,2}A_2$, $^{0,3}A_2$, and $^{0,4}A_2$ cross ring fragments from ion *m/z* 365 $[Hex_2+Na]^+$. This fragmentation pattern suggests that ion $[Hex_2+Na]^+$ contains a reducing end hexose residue substituted at the *O*-6 position.

The ESI-MS/MS spectrum of ion at *m/z* 451 (Fig. 6), attributed to $[dHexPent_2+Na]^+$, showed the presence of ions at *m/z* 319 and 305, identified as $[dHexPent+Na]^+$ and $[Pent_2+Na]^+$, resultant of a loss of 132 Da ($Pent_{res}$) and 146 Da ($dHex_{res}$), respectively. Also present are the ions at *m/z* 301 and *m/z* 287, corresponding to losses of 150 and 164 Da, and identified as $[dHexPent_{res}+Na]^+$ and $[Pent_{2res}+Na]^+$, respectively. The ion present at *m/z* 173 was attributed to $[Pent+Na]^+$. The ions at *m/z* 391 and 361 were attributed to $^{0,2}A_3$ and $^{0,3}A_3$ cross-ring fragments. These results, together with the results of sugars analysis, allowed to conclude that the rhamnose residues are at the non-reducing end and that the arabinosyl residues at the reducing end are substituted on the *O*-5 position.

The presence of rhamnosyl residues as structural features of arabinogalactans has been already described but only as terminally linked to the glucuronic acid residues (Clarke et al., 1979). Although from the data obtained it cannot be excluded the occurrence of rhamnosyl residues linked to glucuronic acid residues in these water soluble coffee arabinogalactans, the oligosaccharides obtained by partial acid hydrolysis clearly show that the rhamnosyl residues are mainly linked to the arabinosyl residues, in the form of trisaccharides in association with two arabinosyl residues, or as disaccharides, in association with a single arabinosyl residue. The presence of terminally linked rhamnosyl residues attached to the arabinosyl residues in coffee arabinogalactans has never been described and, as far as we know, neither on arabinogalactans recovered from other sources.

From the sugar and methylation analysis of the polysaccharide material extracted with hot water from green coffee (Nunes and Coimbra, 2001) it can be deduced that a significant portion (~26%) of the type II arabinogalactans from coffee hot water extract is rhamnoarabinogalactans. The presence of terminally linked rhamnosyl residues in the *O*-5 position of arabinosyl residues can explain the least degradability by the human fecal microbiota of (1 → 5)-linked arabinosyl residues of the coffee arabinogalactans (Gniechwitz et al., 2007).

In order to extend and confirm the results obtained from sugars, methylation, and ESI-MS/MS analysis, the rhamnoarabinogalactans were further studied by 1D and 2D homonuclear and heteronuclear NMR spectroscopy.

2.3. NMR analysis of coffee arabinogalactans

The ^1H NMR spectrum of fraction F1 is shown in Fig. 7. The signals at δ 5.27 and 5.09 ppm were attributed

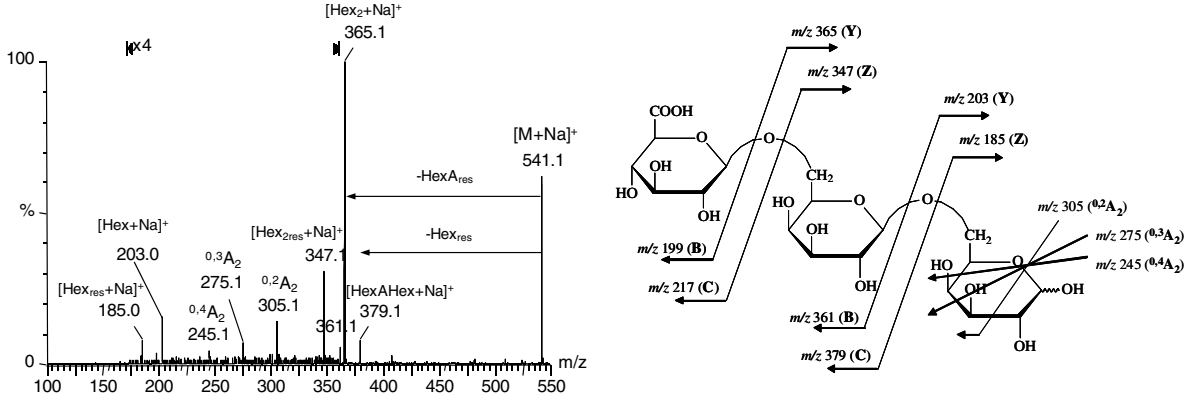

Fig. 5. ESI-MS/MS spectrum of $[M+Na]^+$ adducts of $HexAHex_2$.

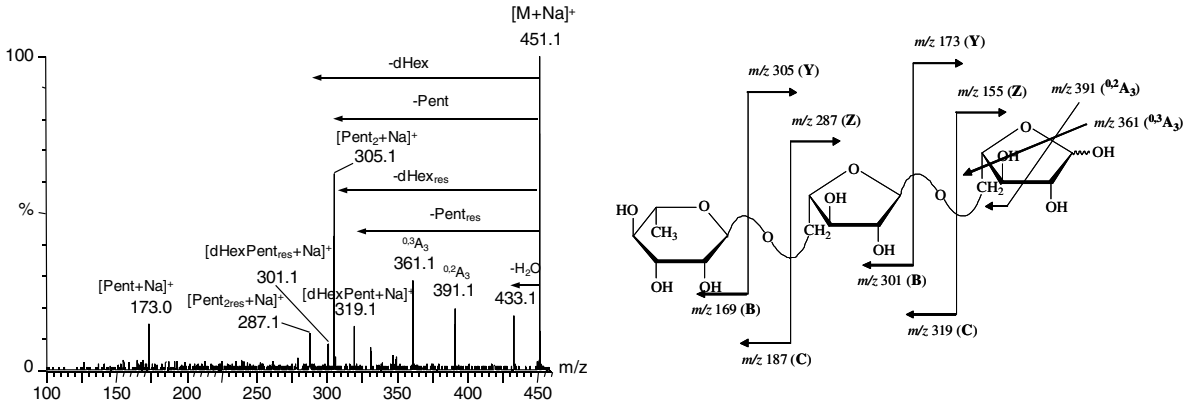

Fig. 6. ESI-MS/MS spectrum of $[M+Na]^+$ adducts of $dHexPent_2$.

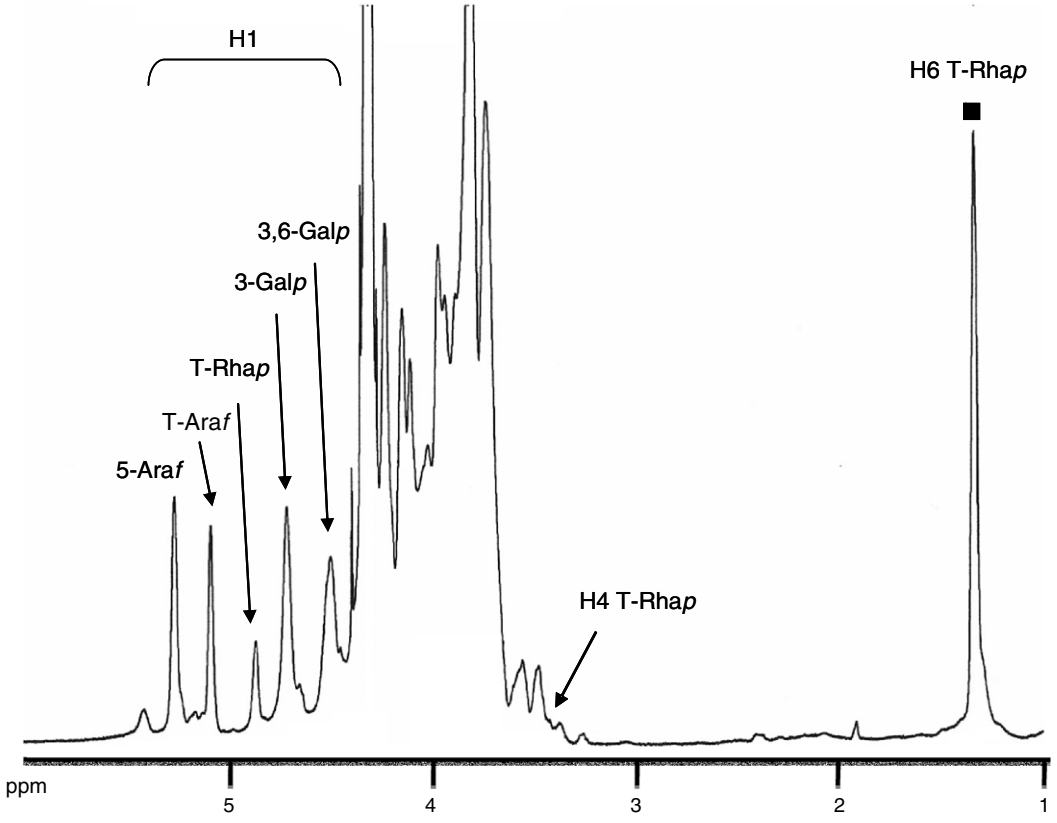

Fig. 7. ^1H NMR spectrum of F1 fraction from hot water soluble green coffee material. (■) also contain a contamination.

to the resonance of H-1 of 5-linked and terminally linked L-arabinofuranosyl residues (Eriksson et al., 1996; Cardoso et al., 2002, 2007; Tan et al., 2004; Dourado et al., 2006). The signal at δ 4.87 ppm was attributed to the terminally linked L-rhamnopyranosyl residues (Tan et al., 2004; Gutiérrez et al., 2005) and the signals at 4.71 and 4.50 ppm were attributed to the 3-linked, and 3,6-linked D-galactopyranosyl residues, respectively (Eriksson et al., 1996; Tan et al., 2004; Gutiérrez et al., 2005). Also, the H-6 signals of the L-rhamnopyranosyl residues were assigned to the signal at δ 1.33 ppm (Tan et al., 2004). From the areas of the H-1 signals in the ^1H NMR spectrum, the relative amount of T-L-Rha*p*:T-L-Ara*f*:(1 → 5)-L-Ara*f*: (1 → 3)-D-Gal*p*: (1 → 3,6)-D-Gal*p* was 1.0:1.5:2.1:2.9:3.0. These values were in close agreement with the values of methylation analysis shown in Table 2.

The one-bond C–H correlation observed in the HSQC spectrum allowed to assign the signals at δ 111.9 ppm to C-1 of 5-linked L-arabinofuranosyl residues, and the signals at δ 110.4–110.8 ppm to C-1 of terminally linked L-arabinofuranosyl residues. The signal at δ 102.7 ppm was attributed to C-1 of L-rhamnopyranosyl residues, and the signals at δ 106.3–106.6 and 106.1 ppm were attributed to C-1 of 3-linked and 3,6-linked D-galactopyranosyl residues,

Table 5
Peak assignments of ^{1}H and ^{13}C NMR spectra of Fraction F1

	1	2	3	4	5 (H_a; H_b)	6 (H_a; H_b)
L-Ara*f*-α-(1→						
^{13}C	110.4–110.8[a]	84.6–84.8[a]	79.5[a,c]	86.9[a,c]	64.2[a,b,c]	
^{1}H	5.09[a]	4.12–4.15[a]	3.95–3.97[a]	4.08–4.11[a]	3.70–3.78;3.82–3.89[a,d]	
→5)-L-Ara^{1}*f*-α-(1→						
^{13}C	111.9[a]	84.6–84.8[a]	79.6[a,c]	86.9[a,c]	69.8[a,b,c]	
^{1}H	5.27[a]	4.20–4.24[a]	4.00–4.03[a]	4.12–4.16[a]	3.75–3.78; 3.85–3.87[a,d]	
→5)-L-Ara^{2}*f*-α-(1→						
^{13}C	111.9[a]	84.6–84.8[a]	79.6[a,c]	85.1[a,c]	69.9[a,b,c]	
^{1}H	5.27[a]	4.20–4.24[a]	4.00–4.03[a]	4.24–4.26[a]	3.80–3.84; 3.87–3.92[a,d]	
L-Rha*p*-α-(1→						
^{13}C	102.7[a]	73.3[a,c]	73.2[a,c]	75.1[a,c]	71.6[a,c]	22.9[a,b,c]
^{1}H	4.87[a]	3.99–4.05[a]	3.79–3.81[a]	3.45–3.49[a]	3.71–3.72[a]	1.33[a]
→3)-D-Gal*p*-β-(1→						
^{13}C	106.3–106.6	73.2	85.1–85.3	71.4	77.5–77.7	63.8
^{1}H	4.71	3.80–3.95	3.83–3.90	4.09–4.12	3.69–3.72	3.79–3.82
→3,6)-D-Gal*p*-β-(1→						
^{13}C	106.1	73.0	82.8–83.6	71.4	76.2–76.4	72.4
^{1}H	4.50	3.67–3.70	3.66–3.72	4.17–4.22	3.89–3.93	3.91–3.99; 4.02–4.09[a,d]

[a] Assignment from COSY and HSQC.
[b] Assignment also from ^{13}C NMR DEPT-135 spectrum.
[c] Assignments confirmed by HMBC.
[d] H_a and H_b, respectively.

respectively (Table 5). These H-1 and C-1 resonances confirm the α configuration of the anomeric carbons for the L-arabinofuranosyl and L-rhamnopyranosyl residues, and β configuration for the anomeric carbons of the D-galactopyranosyl residues (Eriksson et al., 1996; Cardoso et al., 2002; Willfor et al., 2002; Tan et al., 2004; Gutiérrez et al., 2005). The H-6-C-6 cross peaks of the L-rhamnopyranosyl residues were also directly assigned from the HSQC spectrum, being the signal at δ 22.9 ppm attributed to the C-6 carbon of the L-rhamnopyranosyl residues.

The C-5 signals of the 5-linked and terminally linked L-arabinosyl residues and C-6 signals of the 3-linked and 3,6-linked D-galactopyranosyl residues were deduced from the ^{13}C NMR DEPT-135 spectrum (Fig. 8). The signal at δ 64.2 ppm was attributed to the C-5 resonance of the terminally linked L-arabinofuranosyl residues and the signals at δ 69.8 and 69.9 ppm were attributed to the C-5 of the 5-linked L-arabinofuranosyl residues bearing different substituents at the *O*-5 position (Table 5). The signals at δ 63.8 and 72.4 ppm were attributed to the C-6 resonance of the 3-linked and 3,6-linked D-galactopyranosyl residues, respectively. The signal at δ 72.4 ppm was clearly recognizable in the HSQC spectrum (data not shown).

The assignments reported in Table 5 for the other proton and carbon resonances were obtained from 2D homonuclear COSY and heteronuclear HSQC spectra. The ^{13}C assignments were confirmed with help of the ^{13}C DEPT-135 spectrum and with the connectivities found in the 2D HMBC.

From the heteronuclear HMBC spectrum, the linkage sequence of the sugar residues of coffee rhamnoarabinogalactan side chains was determined. The signal at δ 5.09 ppm (H-1 from terminal α-L-Ara*f*) is correlated with the signal at δ 69.9 ppm (C-5 of 5-linked α-L-Ara*f* residues) and also correlated with the signal at δ 72.4 ppm (C-6 of 3,6-linked β-D-Gal*p* residues) and δ 85.1–85.3 ppm (C-3 of 3-linked β-D-Gal*p* residues, Fig. 9). The signal at δ 5.27 ppm (H-1 from 5-linked α-L-Ara*f* residues) is correlated with the signals at δ 82.8–83.6 ppm (C-3 from 3,6-linked β-D-Gal*p* residues). The signal at δ 4.87 ppm (H-1 from terminal α-L-Rha*p* residues) is correlated with signal at δ 69.8 ppm (C-5 from 5-linked α-L-Ara*f* residues, Fig. 9). These results show that the rhamnosyl residues as well as the terminally linked arabinosyl residues are linked to the *O*-5 position of the arabinosyl residues, which are in accordance with the results obtained by ESI-MS/MS. These arabinosyl residues are linked to the *O*-3 position of the 3,6-linked β-D-Gal*p* residues. These results allow to conclude that the β-D-galactosyl residues that contain the arabinosyl side chains belong to a (1 → 6)-linked Gal chain. This conclusion is in accordance with the observed correlation between the signal at δ 4.50 ppm (H-1 of 3,6-linked β-D-Gal*p* residues) and the signal at δ 72.4 ppm (C-6 of 3,6-linked β-D-Gal*p* residues). From these results, it is possible that the terminally linked α-L-Ara*f* residues linked to the *O*-6 position of the 3,6-linked β-D-Gal*p* residues are present as end residues of the (1 → 6) linked β-D-Gal*p* in the side chains. The correlation observed between signal at δ 4.71 ppm (H-1 of 3-linked β-D-Gal*p* residues) with signal at δ 85.1–85.3 ppm can be due to long range C-H coupling constants through H–C–C or H–O–C connectivities.

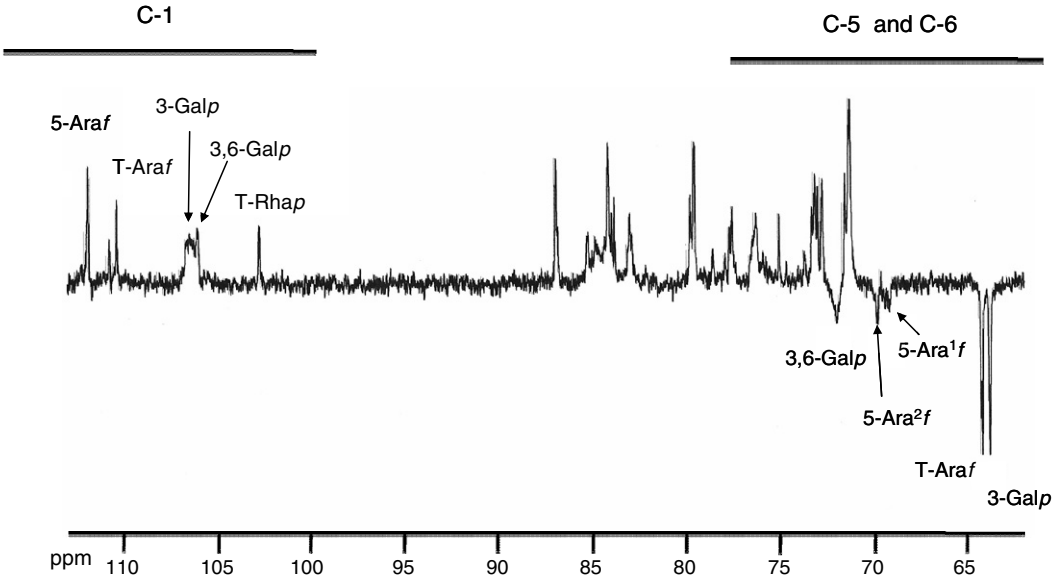

Fig. 8. ^{13}C NMR DEPT-135 spectrum of F1 fraction from hot water soluble green coffee material.

Taking together the results from sugars and methylation analysis with the structural details given by ESI-MS/MS and NMR, the schematic structure presented in Scheme 1 can be proposed for the water soluble coffee rhamnoarabinogalactan. This structure is one of all the possible combinations in terms of size of the (1 → 6)-linked β-D-Gal*p* side chains, interspace in the main (1 → 3)-linked β-D-Gal*p* backbone, and arrangement of the diarabinosyl, rhamnoarabinosyl, and rhamnoarabinoarabinosyl side chains. Nevertheless, this schematic structure summarises, on an approximate molar basis, all the structural details evidenced by methylation, ESI-MS/MS, and NMR analysis discussed in this study.

Taking into account the easy extraction with hot water of these arabinogalactans and their different structural details, these may represent the arabinogalactan population present near the cell lumen of the coffee beans, which were shown to be structurally different from that found throughout the cell walls of coffee beans (Sutherland et al., 2004).

3. Experimental

3.1. Samples and general procedures

The green arabica Brazil coffee (*Coffea arabica*) infusion, the high molecular weight material (HMWM), and the 75% ethanol precipitated fraction (Et75) were obtained as previously described by Nunes and Coimbra (2001). Briefly, with constant stirring, 50 g of ground and defatted green coffee were extracted with 1 l of water at 80 °C for 20 min. The extract was filtered through a size two sintered glass filter, and the material retained was washed with an additional 500 ml of water at 80 °C. The filtrate was concentrated under reduced pressure at 40 °C, and dialysed (MW cut-off 12–14 kDa, Visking size 8, Medicell International Ltd., London, UK) at 4 °C with eight water renewals. The retentate obtained was frozen and freeze-dried, giving the HMWM. The HMWM (1.0 g) was dissolved in 100 ml of water; the solution was stirred for 1 h at 4 °C and centrifuged at 24,400*g* for 20 min at 4 °C. Absolute ethanol (Riedel, Seelze, Germany, 100 ml) was added to the supernatant and the solution (50% ethanol, assuming additive volumes) was stirred for 1 h at 4 °C. This solution was then centrifuged and the residue obtained was removed. To the new supernatant was added 200 ml of absolute ethanol; the solution (75% ethanol) was stirred for 1 h at 4 °C and centrifuged, and the residue obtained (Et75) was removed from the supernatant solution. To remove the ethanol completely, each precipitate was dissolved in water, concentrated by rotary evaporation at 40 °C, and then freeze-dried.

The sugars were determined by gas chromatography as alditol acetates after hydrolysis with 1 M sulfuric acid at 100 °C during 2.5 h or by hydrolysis with TFA 2 M at 120 °C during 1 h. Uronic acids were determined colorimetrically according to a modification (Coimbra et al., 1996) of the method of Blumenkrantz and Asboe-Hansen (1973).

The methylation procedure to obtain the partially methylated alditol acetates and the analysis by GC–MS were performed as previously described (Nunes and Coimbra, 2001). Methanolysis was performed according to the procedure described by Bleton et al. (1998). Briefly, 2 ml of anhydrous methanol:HCl 0.5 M were added to 2 mg of polysaccharides. The mixture was heated during 16 h at 90 °C and, after cooling, the reagent was removed under a stream of nitrogen at 40 °C. The residue was derivatised by addition of 0.5 ml of hexadimethyl-silazane:pyridine:trimethylchlorosilane (9:3:1) during 1 h at 80 °C. After

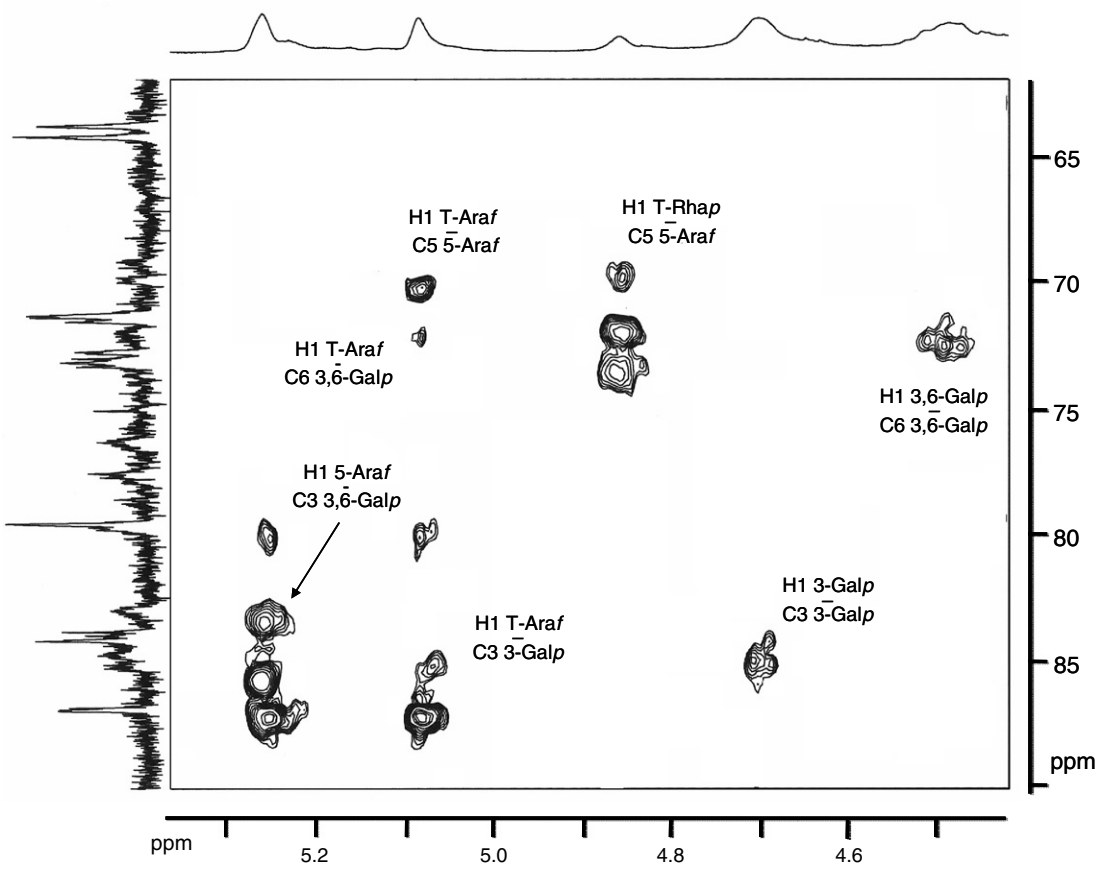

Fig. 9. HMBC spectrum of F1 fraction from hot water soluble green coffee material.

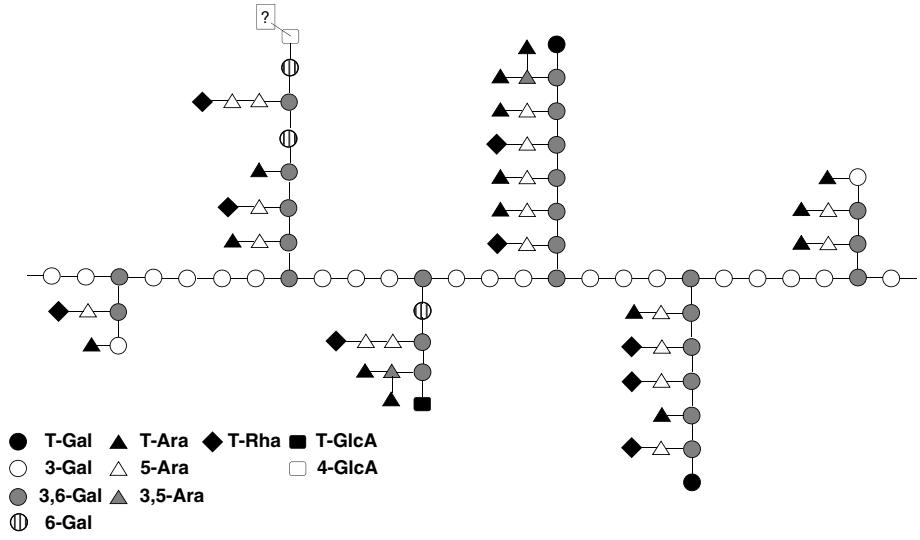

Scheme 1. One of many possible structural arrangements for the carbohydrate moiety of arabinogalactan-protein F1 isolated by hot water extraction of green coffee.

cooling to room temperature, the silyl derivatives were analysed by GC–MS (Agilent, USA) using a DB-1 column (30 m length, 0.23 mm internal diameter, and 0.2 μm film thickness) injecting 1 μl in splitless mode (time of splitless 0.75 min). Both the injector and the transfer line were set at 260 and 250 °C, respectively. The initial temperature of the column was 120 °C and held for 1 min, increasing 2 °C/min until 230 °C. The MS source temperature was

set at 180 °C and the electron ionization energy was set at 70 eV, with scans from m/z 40 to 600.

Protein content was determined after acid hydrolysis with 6 M HCl during 24 h. After removing the acid by centrifugal evaporation (Univapo 100 ECH, UniEquip, Munich, Germany) at 40 °C under vacuum, the solid residue was dissolved in 3 ml of 0.1 M HCl and filtered through a 45 μm pore size membrane. Amino acids were determined by GC–FID after derivatisation as heptafluorobutylisobutyl derivatives (MacKenzie, 1987).

3.2. Anion exchange chromatography

Anion exchange chromatography was performed on a Q-Sepharose FF stationary phase (loaded on a C10/10 column, Pharmacia). The eluent was a pH 6.5 Na-phosphate 100 mM buffer containing 3 M urea and 0.02% sodium azide. Et75 fraction (1 mg/ml) was applied to the column and, after application, the column was flushed with a minimum of 4 column volumes of the initial buffer or until the absorbance at 280 nm reached the initial level. The retained material was eluted with buffer containing 3 M urea and 1 M NaCl. Fractions (2 ml) were collected and assayed for sugars by the phenol–sulfuric acid method and continuously monitored at 280 nm. The appropriated fractions were polled, dialysed (12–14 kDa cut-off), and freeze-dried.

3.3. Size exclusion chromatography

Size exclusion chromatography on Sephacryl S-300 HR was performed on a column width of 2.6 and 70 cm length (XK 26/70, Pharmacia) at a flow rate of 0.3 ml/min. Samples (2 mg) were suspended in 1 ml of 100 mM Na phosphate buffer, pH 6.5, containing 3 M urea. The same phosphate/urea buffer was used as the eluent. Fractions (1 ml) were collected and assayed for sugars with the phenol–H_2SO_4 method, and the eluent was continuously monitored at 280 nm. Exclusion and total volumes were calibrated with Blue Dextran and Glc, respectively.

Size exclusion chromatography on Biogel P-30 was performed on a XK 1.6/100 column containing Biogel P-30 with a flow rate of 0.1 ml/min. The freeze-dried material was dissolved in 2 ml of 100 mM pyridine–acetate buffer, pH 5.3, and loaded on the column previously equilibrated with the loading buffer. Exclusion and total volume were calibrated with Blue Dextran and Glc, respectively. Fractions (1 ml) were collected and assayed for sugars with the phenol–H_2SO_4 method. The appropriated fractions were pooled and rotary evaporated until all the buffer was removed by repeated additions of distilled water and then was freeze-dried.

3.4. β-Yariv precipitation assay for arabinogalactan-proteins

Fifteen microliters of F1 fraction (4 mg/ml of 0.15 M NaCl and 0.2% sodium azide) were poured in spots of 4 mm width made on a ~3 mm thick agarose gel (1%) containing the Yariv reagent (0.002%), 0.15 M NaCl, and 0.02% sodium azide, in Petri dishes. The reagents without polysaccharide were used as blanks and gum arabic arabinogalactan was used as positive test polysaccharides. The Petri dishes were sealed with parafilm and left in the dark at room temperature for 2 days to allow the coloured halo to develop (Redgwell et al., 2002).

3.5. Partial acid hydrolysis

For the partial acid hydrolysis of fraction F1, 2 ml of 50 mM trifluoroacetic acid were added to 10 mg of polysaccharide and the hydrolysis was performed during 30 min at 70 °C. After separation of the polymeric material by size exclusion chromatography on Biogel-P30, the solvent was removed by centrifugal evaporation (Univapo 100 ECH, UniEquip, Munich, Germany) at 40 °C under vacuum. Two ml of 250 mM TFA was added to the solid residue and the mixture was hydrolysed at 70 °C during 30 min.

3.6. Electrospray ionization mass spectrometry

The freeze-dried fractions obtained from the Biogel P-30 column were dissolved in 200 μl of 1:1 methanol–water solution containing 1% (v/v) formic acid in a concentration of approximately 0.25 mg/ml. Samples were introduced into the mass spectrometer using a flow rate of 10 μl/min. Positive ion ESI-MS and MS/MS spectra were acquired using a Q-TOF 2 instrument (Micromass, Manchester, UK), setting the needle voltage at 3000 V with the ion source at 80 °C and cone voltage at 35 V (Reis et al., 2002). Each spectrum was produced by accumulating data during approximately 1–2 min. MS/MS spectra of $[M+Na]^+$ ions were obtained by collision induced dissociation (CID), using argon as the collision gas and varying collision energy between 40 and 50 eV. In MS and MS/MS experiments, TOF resolution was set at approximately 10,000 (full width between half-maximum peaks-FWHM definition). In MS/MS experiments Q1 peak width (FWHM) was set at approximately 0.7 Th.

3.7. NMR analysis

^1H and ^{13}C NMR spectra were recorded in D_2O on a Bruker Avance 500 spectrometer operating at 500.13 and 125.77 MHz, respectively; the chemical shifts are expressed in δ (ppm) values relative to TSS (sodium salt of 3-(trimethylsilyl)-1-propane-d_4-sulfonic acid) as external reference. 2D COSYPR (homonuclear shift correlation with presaturation during relaxation delay) spectrum was recorded with 200 transients over 256 increments (zero-filled to 1 K) and 1 K data points with spectral widths of 3000 Hz. The repetition time was 1.8 s. These data were processed in the absolute-value mode. The phase sensitive ^1H-detected (^1H, ^{13}C) gHSQC (heteronuclear single quantum coherence, using gradient pulses for selection) spectrum was recorded with 200 transients over 256 increments (zero-filled to 1 K) and

1 K data points with spectral widths of 3500 Hz in F2 and 13,200 Hz in F1. The repetition time was 2.3 s. A cosine multiplication was applied in both dimensions. The delays were adjusted according to a coupling constant ^1J(CH) of 149 Hz. The *g*HMBC (heteronuclear multiple quantum coherence, using gradient pulses for selection) spectrum was recorded with 200 transients over 256 increments (zero-filled to 1 K) and 1 K data points with spectral widths of 3500 Hz in F2 and 13,200 Hz in F1. The repetition time was 2.3 s. A sine multiplication was applied in both dimensions. The low-pass *J*-filter of the experiment was adjusted for an average coupling constant ^1J(CH) of 149 Hz and the long-range delay utilised to excite the heteronuclear multiple quantum coherence was optimised for 7 Hz. The spectrum was acquired at 40 °C.

Acknowledgement

The authors gratefully acknowledge Professor Henk A. Schols (Wageningen, The Netherlands) for kindly providing the Yariv Reagent, FCT-Portugal for the financial support to the project POCI/QUI/59337/2004, to the Research Unit of Chemistry, Vila Real, and the Research Unit 62/94 "Química Orgânica, Produtos Naturais e Agro-Alimentares", Aveiro, and the financial support of FEDER.

References

Bleton, J., Mejanelle, P., Sansoulet, J., Goursaud, S., Tchapla, A., 1998. Characterization of neutral sugars and uronic acids after methanolysis and trimethylsilylation for recognition of plant gums. J. Chromatogr. A 720, 27–49.

Blumenkrantz, N., Asboe-Hansen, G., 1973. New method for quantitative determination of uronic acids. Anal. Biochem. 54, 484–489.

Bradbury, A.G.W., 2001. Carbohydrates. In: Clarke, R.J., Vitzthum, O.G. (Eds.), Coffee Recent Developments. Blackwell Science, Oxford, pp. 1–17.

Cardoso, S.M., Silva, A.M.S., Coimbra, M.A., 2002. Structural characterization of the olive pomace pectic polysaccharide arabinan side chains. Carbohydr. Res. 337, 917–924.

Cardoso, S.M., Ferreira, J.A., Mafra, I., Silva, A.M.S., Coimbra, M.A., 2007. Structural ripening-related changes of the arabinan-rich pectic polysaccharides from olive pulp cell walls. J. Agric. Food Chem. 55, 7124–7130.

Chapman, A., Blervacq, A.-S., Vasseur, J., Hilbert, J.-L., 2000. Arabinogalactan-proteins in *Cichorium* somatic embryogenesis: effects of β-glucosyl Yariv reagent and epitope localisation during embryo development. Planta 211, 305–314.

Clarke, A.E., Anderson, R.L., Stone, B.A., 1979. Form and function of arabinogalactans and arabinogalactan-proteins. Phytochemistry 18, 521–540.

Coimbra, M.A., Delgadillo, I., Waldron, K.W., Selvendran, R.R., 1996. Isolation and analysis of cell wall polymers from olive pulp. In: Linskens, H.F., Jackson, J.F. (Eds.), Modern Methods of Plant Analysis, vol. 17. Springer-Verlag, Berlin, pp. 19–44.

Ding, L., Zhu, J.K., 1997. A role for arabinogalactan-proteins in root epidermal cell expansion. Planta 203, 289–294.

Domon, B., Costello, C.E., 1988. A systematic nomenclature for carbohydrate fragmentations in FAB–MS–MS spectra of glycoconjugates. Glycoconj. J. 5, 397–409.

Dourado, F., Cardoso, S.M., Silva, A.M.S., Gama, F.M., Coimbra, M.A., 2006. NMR structural elucidation of the arabinan from *Prunus dulcis* immunobiological active pectic polysaccharides. Carbohydr. Polym. 66, 27–33.

Eriksson, I., Andersson, R., Westerlund, E., Andersson, R., Aman, P., 1996. Structural features of an arabinan fragment isolated from the water-soluble fraction of dehulled rapseed. Carbohydr. Res. 281, 161–172.

Fischer, M., Reimann, S., Trovato, V., Redgwell, R.J., 2001. Polysaccharides of green Arabica and Robusta coffee beans. Carbohydr. Res. 330, 93–101.

Gao, M., Kieliszewski, M.J., Lamport, D.T.A., Showalter, A.M., 1999. Isolation, characterization and immunolocalization of a novel modular tomato arabinogalactan-protein corresponding to the LeAGP-1 gene. Plant J. 18, 43–55.

Gniechwitz, D., Reichardt, N., Blaut, M., Steinhart, H., Bunzel, M., 2007. Dietary fiber from coffee beverage – degradation by human fecal microbiota. J. Agric. Food Chem. 55, 6989–6996.

Gutiérrez, O.G., Martinéz, M., Sanabria, L., de Pinto, G.L., Igatuburu, J.M., 2005. 1D and 2D spectroscopy studies of the polysaccharide gum from *Spondias purpurea* var. *lutea*. Food Hydrocolloid 19, 37–43.

Josè-Estanyol, M., Puigdomènech, P., 2000. Plant cell wall glycoproteins and their genes. Plant Physiol. Biochem. 38, 97–108.

Knox, J.P., Linstead, P.J., Peart, J., Cooper, C., Roberts, K., 1991. Developmentally regulated epitopes of cell surface arabinogalactan proteins and their relation to root tissue pattern formation. Plant J. 1, 317–326.

Kreuger, M., van Holst, G.-J., 1993. Arabinogalactan-proteins are essential in somatic embryogenesis of *Daucus carota* L.. Planta 189, 243–248.

MacKenzie, S.L., 1987. Gas chromatographic analysis of amino acids as the *N*-heptafluorobutyryl isobutyl esters. J. Assoc. Off. Anal. Chem. 70, 151–160.

Nunes, F.M., Coimbra, M.A., 2001. Chemical characterization of the high molecular weight material extracted with hot water from green and roasted Arabica coffee. J. Agric. Food Chem. 49, 1773–1782.

Nunes, F.M., Domingues, M.R., Coimbra, M.A., 2005. Arabinosyl and glucosyl residues as structural features of acetylated galactomannans from green and roasted coffee infusions. Carbohydr. Res. 340, 1689–1698.

Pennell, R.I., Roberts, K., 1990. Sexual development in the pea is presaged by altered expression of arabinogalactan protein. Nature 344, 547–549.

Redgwell, R., Curti, D., Fischer, M., Nicola, P., Fay, L., 2002. Coffee arabinogalactans: acidic polysaccharides covalently linked to proteins. Carbohydr. Res. 337, 239–253.

Reis, A., Coimbra, M.A., Domingues, P., Ferrer-Correia, A.J., Domingues, M.R.M., 2002. Structural characterisation of underivatised olive pulp xylo-oligosaccharides by mass spectrometry using matrix assisted laser desorption/ionisation and electrospray ionisation. Rapid Commun. Mass Spectrom. 16, 2124–2132.

Selvendran, R.R., Ryden, P., 1990. Isolation and analysis of plant cell walls. In: Dey, P.M. (Ed.), Methods in Plant Biochemistry, vol. 2. Academic Press, pp. 549–570.

Serpe, M.D., Nothnagel, E.A., 1994. Effects of Yariv phenylglycosides on *Rosa* cell suspensions: evidence for the involvement of arabinogalactan-proteins in cell proliferation. Planta 193, 541–550.

Simões, J., Domingues, P., Reis, A., Nunes, F.M., Coimbra, M.A., Domingues, M.R.M., 2007. Identification of anomeric configuration of underivatized reducing glucopyranosyl-glucose disaccharides by tandem mass spectrometry and multivariate analysis. Anal. Chem. 79, 5896–5905.

Sommer-Knudsen, J., Bacic, A., Clarke, A.E., 1998. Hydroxyproline-rich plant glycoproteins. Phytochemistry 47, 183–497.

Sutherland, P.W., Hallett, I.C., MacRae, E., Fischer, M., Redgwell, R.J., 2004. Cytochemistry and immunolocalisation of polysaccharides and proteoglycans in the endosperm of green arabica coffee beans. Protoplasma 223, 203–211.

Tan, L., Qiu, F., Lamport, D.T.A., Kieliszewski, M.J., 2004. Structure of a hydroxyproline (Hyp)-arabinogalactan polysaccharide from repetitive Ala–Hyp expressed in transgenic *Nicotiana tabacum*. J. Biol. Chem. 279, 13156–13165.

Thompson, H.J.M., Knox, J.P., 1998. Stage-specific responses of embryogenic carrot cell suspension cultures to arabinogalactan protein-binding β-glucosyl Yariv reagent. Planta 205, 32–38.

van Holst, G.-J., Clarke, A.E., 1985. Quantification of arabinogalactan-protein in plant extracts by single radial gel diffusion. Anal. Biochem. 148, 446–450.

Willats, W.G.T., Knox, J.P., 1996. A role for arabinogalactanproteins in plant cell expansion: evidence from studies on the interaction of β-glucosyl Yariv reagent with seedlings of *Arabidopsis thaliana*. Plant J. 9, 919–925.

Willfor, S., Sjoholm, R., Laine, C., Holmbom, B., 2002. Structural features of water-soluble arabinogalactans from Norway spruce and scots pine heartwood. Wood Sci. Technol. 36, 101–110.

Zaia, J., 2004. Mass spectrometry of oligosaccharides. Mass Spectrom. Rev. 23, 161–227.